Precise Measurement of the W-boson with the Collider Detector at Fermilab

Supervisor: Chris Hays Candidate Number: 446710 OSS Student Identification Number: 473122

The most precise measurement of the mass of the W-boson to date has been the measurement $M_w = 80\,387 \pm 12_{stat} \pm 15_{syst} = 80\,387 \pm 19$ MeV using a $\sqrt{s}$ = 1.96 TeV proton-antiproton collider and the CDFII detector[1]. Using the POWHEG NLO-QCD event generator in conjunction with the global PDF sets CT10 and MSTW68, we can produce a sample of Monte Carlo events as input to a custom detector model simulation of the CDFII experiment. We study the PDF uncertainties on the W mass and compare with those of other measureable quantities such as Z rapidity and the W charge asymmetry as a function of rapidity. These studies suggest several strategies for reducing the PDF uncertainties on the CDF measurement of M_W below the current value of 10 MeV.

I. Introduction

The mass of W Boson, M_W, is an important parameter in the standard model of particle physics. A precise measurement of M_W tests the consistency of the standard model, as M_W is sensitive to the values of other standard model parameters such as the mass of the Higgs boson. At the CDFII experiment, proton-antiproton collisions were produced at a centre of mass energy of $\sqrt{s}$ = *1.96 TeV*. The collisions which produce W bosons do so primarily through the s-channel annihilation of valence quarks[2]. The W boson can then decay to a lepton and neutrino, as shown in Figure 1, or to a quark-antiquark pair. By measuring the 4-momenta of the charged lepton and the hadronic recoil of the reaction, M_W can be indirectly measured. The uncertainties in the CDF measurement can be categorised by source. Table 1 shows that one of the largest sources of error is the uncertainty on the parton distribution functions (PDFs). Parton distribution functions describe the fractional momentum distribution of partons within a proton, an example of which is shown in Figure 2.

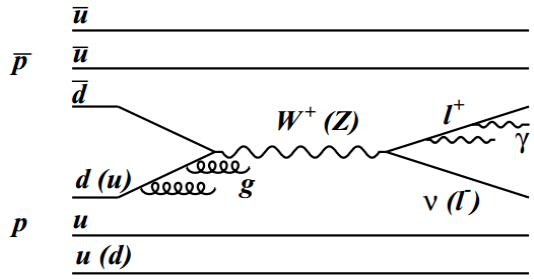

Figure 1: *The production and leptonic decay of a W (or Z) boson in a proton-antiproton collision.[2]*

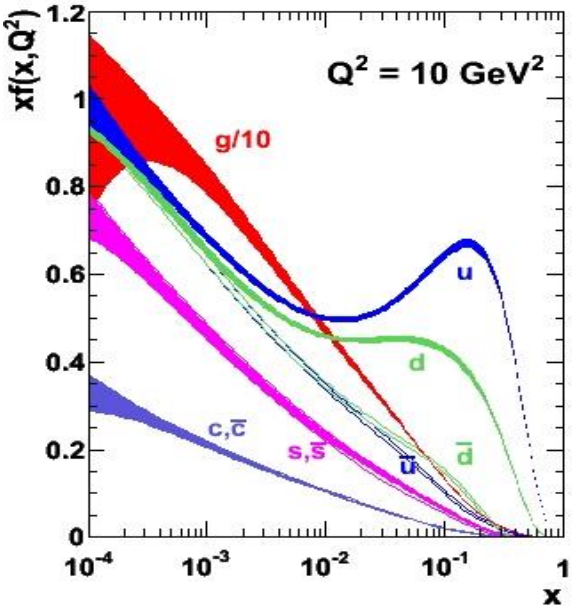

Figure 2: *A graphical representation of the central PDF of the MTSW (2008) set at a momentum-square transfer (Q^2) of 10GeV. The distribution of momentum within the proton shifts between the partons as a function of x, a dimensionless variable defined as $Q^2/2Mv$ where v is the energy loss of the scattered particle, and M is the mass of the target nucleon. In the elastic limit (as x tends to 1) the momentum is distributed almost entirely between the up and down quarks with the focus shifting to gluons and heavier quarks as x decreases.* [3]

Source of uncertainty	Uncertainty (MeV)
Lepton energy scale and resolution	7
Recoil energy scale and resolution	6
Lepton removal	2
Backgrounds	3
P_T(W) model	5
Parton distributions	10
QED radiation	4
W-boson statistics	12
Total	19

Table 1: *Uncertainties on the final combined result on M_w*[1]

The sets of PDFs we investigated are shown in Table 2. In this paper, I first the detail the model used to generate W and Z events, as well as the criteria used to select W and Z events from the background. I then describe the detector model used to accurately represent the capabilities of the CDF detector. Finally I describe the validations performed through comparisons with the results of the CDFII experiment and the strategies investigated to constrain the PDF uncertainties.

PDF set range	members	LHAPDF set prefix
11000-11052	52 + 1	CT10nlo
21100-21140	40 + 1	MSTW2008nlo68cl
21141-21180	40 + 1	MSTW2008nlo90cl
229800-22900	100	NNPDF23nloas0118
230200-230300	100	NNPDF23nloas0120

Table 2: *The PDF sets and the PDF numbers used in this project. LHAPDF is the standard PDF library*[4]

II. Overview

A. Definitions

We use a right-handed coordinate system with the z-axis tangential to the proton beam and centred at the middle of the detector. Transverse quantities such as the transverse momentum of the lepton, p_T^l, are projections onto the x–y plane. We define the azimuthal angle $\phi \equiv \tan^{-1}(y/x)$. Pseudorapidity is defined as $\eta = -\ln[\tan(\Theta/2)]$ where Θ is the polar angle from the Z axis. We use the convention $\bar{h}$ = c = 1 throughout this paper.

B. Measurement strategy

The primary challenge in precisely measuring M_W at a hadron collider is that only one of the decay products of the W-boson, the neutrino, interacts solely through the weak force, and therefore escapes the detector without leaving any signal. This makes it impossible to calculate the 4-momentum of the W-boson merely by summing the 4-momenta of its decay products. In the case of the Z however, the decay products both have non-zero charge, so the 4-momentum of the boson can be measured directly. When a boson is produced in a hadronic collision such as the proton-antiproton collisions at the CDF, there is some hadronic recoil (U) providing momentum to the boson in the transverse plane (Figure 3). By measuring this hadronic recoil and comparing it with the transverse momentum of the Z-boson for each event, we can construct and tune a model for reconstructing the W-boson transverse momentum from the hadronic recoil, and lepton momenta alone (Figure 4). By imposing conservation of momentum and combining with the charged lepton transverse

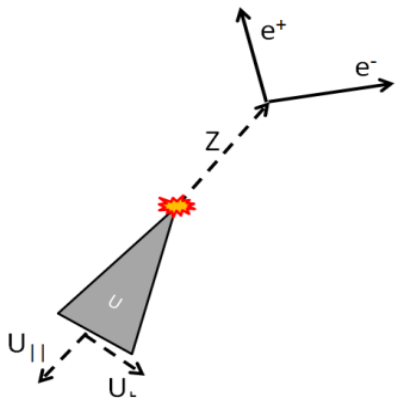

Figure 3: *A Z-boson event, with the hadronic recoil momentum separated into components antiparallel ($U_{||}$) and Perpendicular (U_L) to the Z-boson Transverse momentum.*

momentum we can infer the transverse momentum of the undetected neutrino.

$$p_T^{\nu} = -(p_T^{l} + U_T) \qquad (1)$$

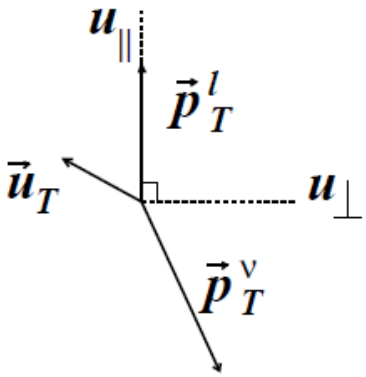

Figure 4: *A W-boson event with the hadronic recoil momentum separated into components parallel ($U_{//}$) and perpendicular ($U_{\perp}$) to the charged lepton transverse momentum.* [2]

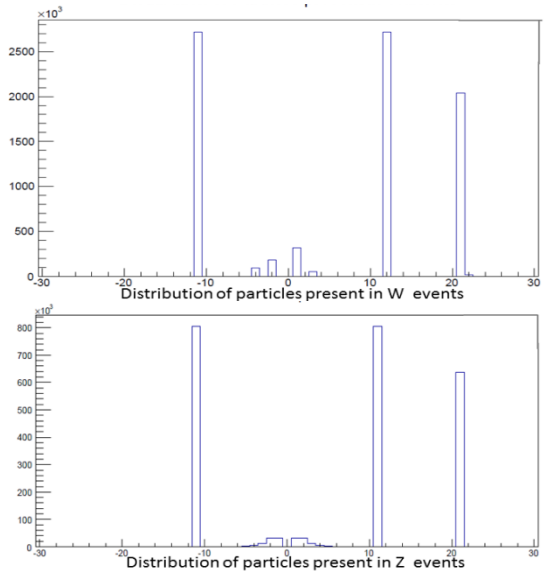

Figure 5: *A histogram comparing the distribution of particles produced by POWHEG for W (top) and Z (bottom) events. The numbers on the x-axis correspond to the LHAPDF particle ID convention*[4].

C. POWHEG event generation process

To model the proton-antiproton collisions, 366 million W^+ events and 100 million W^- events were constructed using the next-to-leading order in quantum chromodynamics event generator, POWHEG[5]. POWHEG models the single emission of a quark or gluon in the initial state with a leading order calculation and a next-to-leading logarithmic correction to the momentum of the parton. This is an improvement on the leading-order generators used in previous valuations of PDF uncertainties by the CDF experiment[2]. We additionally produced 300 million Z events with POWHEG for separate PDF and detector modelling studies. The events were then re-weighted for each of the PDF sets in Table 2. POWHEG outputs the 4-momenta of the leptons and up to one radiated quark or gluon. Figure 5 shows a representative sample of the distribution of the particles in the events produced by POWHEG for both the W^+ and Z events.

In W^+ events, the majority of the particles detected are neutrinos (12), positrons (-11), and gluons (21), with a small amount of quarks (1 to 5), antiquarks (-1 to -5) and photons (22). For Z events the primary products are electrons (11), positrons, gluons and some quarks and antiquarks.

D. The Detector Model

All detectors are subject to inevitable experimental limitations in the measurement of particle momenta, and these limitations amount to a large part of the uncertainty in the measurement of M_W. Therefore, data from POWHEG is processed through a detector model. The detector model is a series of smearing functions designed to obscure the physical quantities in the same way in which we would expect a particle detector to do so. First, we apply a Gaussian smearing function to the transverse momentum of the electron to account for calorimeter resolution[6]. The smearing is calculated as shown in equation (1).

$$\frac{\sigma_E}{P_T^l} = \sqrt{\frac{0.126^2}{p_T^l} + C^2} \qquad (1)$$

Fraction	Value of C
5%	0.013
45%	0.0095
5%	0.03
45%	0.028

Table 3: *The Values of C used for the Gaussian smearing of the charged lepton(s).*

The value for C varies according to the distribution given by Table 3, to model following phenomena: We estimate that in 50% of events the lepton radiates a high energy photon, degrading the resolution in the calorimeter. We also estimate that 10% of the time, electron showers will leak into the gap between the two calorimeter towers nearest zero rapidity, and we degrade the resolution accordingly in these cases. Another source of experimental uncertainty is the electron leakage in the calorimeter. A typical 50 GeV electron will deposit only around 95% of its energy in the calorimeter, with the remaining 5% leaking out of the back. Studies have shown that a gamma distribution $\Gamma(x) = x^a e^{-x}$ where $x \equiv (log_{10} f + \mu)/\sigma$ gives a good approximation of the fractional electron leakage, f, for an electron within the 30 GeV<p_T^l<55 GeV energy range with the parameters set to a=5 σ=0.07 and μ=1.8[7]. We thus calculate the electron leakage correction shown in Figure 6 as:

$$\Delta p_T^l = x^5 e^x (p_T^l) \qquad (2)$$

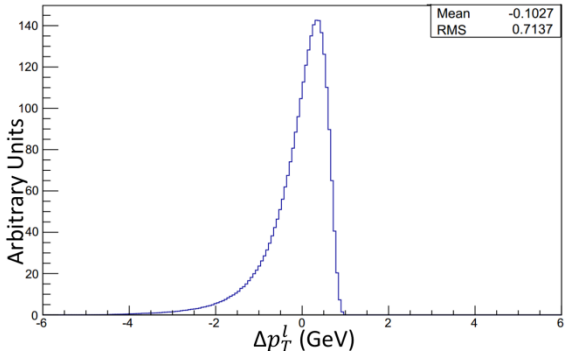

Figure 6: *The leakage correction which is applied to the transverse momentum of the lepton(s)*

This leakage correction is then subtracted from the reconstructed transverse momentum of the lepton once it has been shifted up by 15.61 MeV such that the mean correction from the function is zero. We scale the U_T generated by POWHEG by a factor of 0.65 to account for the fact that the response of the calorimeter to the hadronic recoil is 65%[6]. Gaussian smearing is then applied to the hadronic recoil with a distribution of $\sigma_U = 0.8\sqrt{U_T}$.

We add a flat smearing parameter, $F_{Angular}$, to the angle of the lepton(s) whose bounds decrease linearly as a function of the momentum of U in the transverse plane, U_T up to U_T =15 GeV,

$$F_{Angular} \leq 0.5 * \sqrt{12} * [0.5 - (0.3\frac{U_T}{15})] \text{ Radians} \qquad (3)$$

for U_T<15GeV,

$$F_{Angular} \leq 0.5 * \sqrt{12} * [0.2] \text{ Radians} \qquad (4)$$

for U_T>15GeV

such that the relative resolution on the angle improves with the relative resolution on the recoil.

In a proton-antiproton collision, a fraction of the energy is absorbed in breaking up the hadrons. This underlying event energy is then radiated spherically symmetrically in the form of gluons. To model the underlying event energy, a vector is added at a randomised angle to the vector of the Recoil with a magnitude given by a Gaussian distribution with $\sigma_{Underlying\ Energy}$ = 5.1 GeV.[6] The derivation of our values for the magnitude of the angular smearing and underlying event energy is described in the calibration section. In the CDF experiment, data from seven of the hadronic calorimeter towers which were in the direct path of the lepton beam were not taken into account, because interference from the lepton beam caused unreasonably large readings[2]. Data from neighbouring hadronic calorimeter towers show a reading of around 30 MeV per tower. We therefore decrease the hadronic recoil of our detector model by 200MeV along the direction of the lepton.

E. Criteria for selection of W and Z boson events.

The selected W events are required to pass the same criteria as in the CDF measurement. Two requirements are 30 GeV < p_T^l < 55 GeV and 30 GeV < p_T^ν <55 GeV because in a W decay both the lepton and neutrino will have a transverse momentum of roughly half that of the W-boson. Using the knowledge that the W-boson has a mass in the region of ~80 GeV[8], we expect leptons or neutrinos with transverse momentum of less than 35 GeV or greater than 55 GeV to have poorer mass resolution, or to have occurred either as result of background. We also require 60 GeV < transverse mass < 100 GeV[1], where the transverse mass, M_T is defined as[8];

$$M_T = \sqrt{2p_T^l p_T^\nu [1 - \cos(\phi^l - \phi^\nu)]} \qquad (5)$$

where $(\phi^l - \phi^\nu)$ is the azimuthal angle between the neutrino and the charged lepton. We also require that the pseudorapidity $|\eta|$<1 and that the transverse recoil U_T < 15 GeV[1], as this ensures that the W-bosons have their centre of momentum frame roughly consistent with the lab frame in the transverse plane.

When selecting Z events, we have the benefit of being able to calculate the invariant mass from the four-vector of the lepton-antilepton pair. We therefore require 66 GeV < invariant Mass < 116 GeV[9], centred on M_Z = 91.188 GeV[8]. We also cut on electron and positron transverse momenta 30 GeV<p_T^l<65 GeV where the increased upper bound for p_T^l reflects the higher mass of the Z boson. For consistency with the W, we also apply cuts on pseudorapidity $|\eta|$<1 and Z_T<30 GeV[1].

F. Calibration of the model to the experimental data

In order to replicate the resolution capabilities of the Detector at CDF, we must tune the smearing parameters on our detector model such as the underlying event energy and the angular smearing function. We plot the root mean squared spread of the sum of all 4-momenta in the directions parallel (Figure 7) and perpendicular (Figure 8) to the Z-boson, over a range of P_T of the Z-boson to obtain measurements to the resolution in each of these directions. We tune the parameters in our detector model such that the resolution as predicted by our model fits closely with the resolution of the CDF[2]. By this method we arrive at values for underlying energy of 5.1GeV and the semi-linear angular smearing bounds in equations (3) and (4).

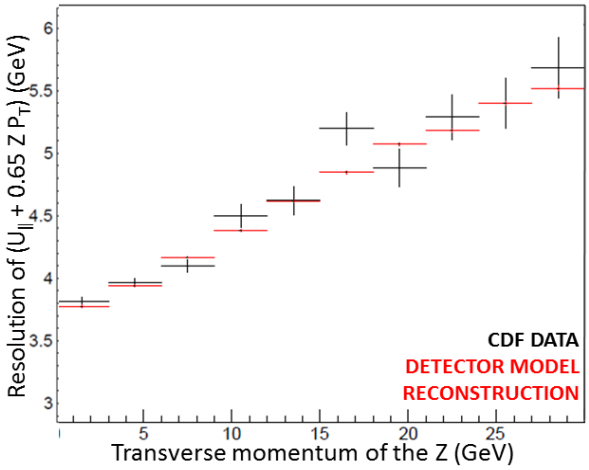

Figure 7: *The tuned detector model compared to CDF data for the resolution on the recoil perpendicular to the Z-boson P_T.*

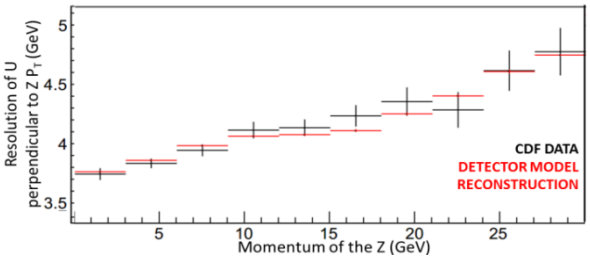

Figure 8 *The tuned detector model compared to CDF data for the resolution on the recoil perpendicular to the Z-boson. There is some inflection in the model at U_T=15GeV where the angular smearing changes from a linear to a flat U_T Dependence.*

G. Model Tests

To test the accuracy of our model, we check the model's prediction of several important quantities by comparing to data from the CDF.

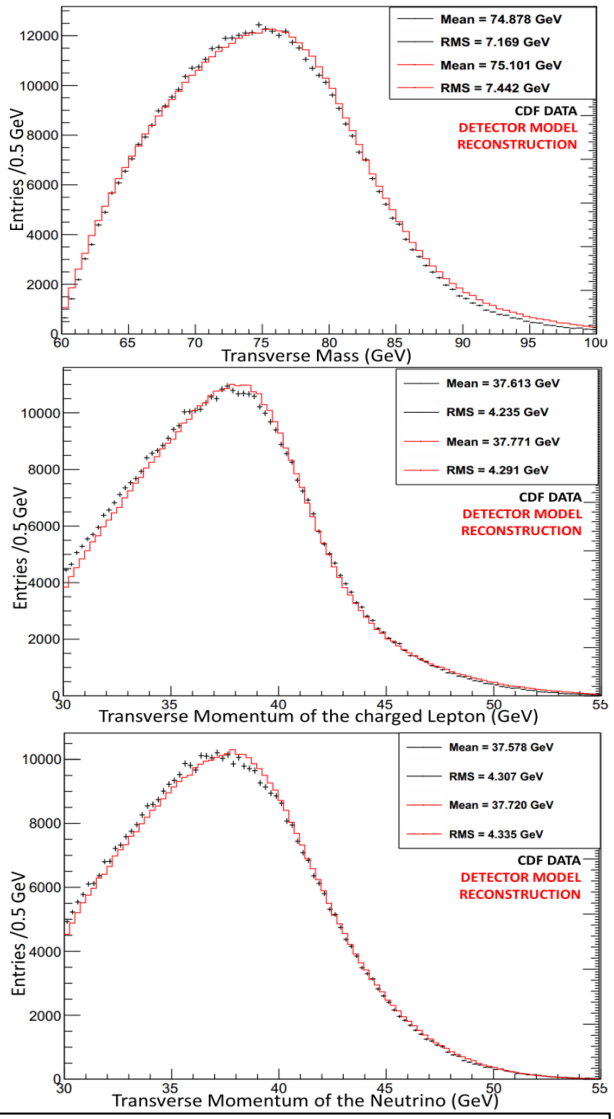

Figure 9: *The transverse mass (top), charged lepton P_T (centre) and neutrino P_T (bottom) detector model reconstructions compared to the CDF data*[1] *. The close fits to the data serve as an important check on the quality of our model.*

Quantities we compare included electron and neutrino transverse mass, and the transverse mass of the W-boson these comparisons are shown in Figure 9. Figure 10 shows our checks that the recoil of the W-boson scales properly with U_T in the direction parallel to the charged lepton, and Figures 11 and 12 show checks on the resolution hadronic recoil in the directions parallel and perpendicular to the lepton P_T respectively. Comparing plots for the invariant mass of the Z-boson (Figure 13) with that from CDF data also tests

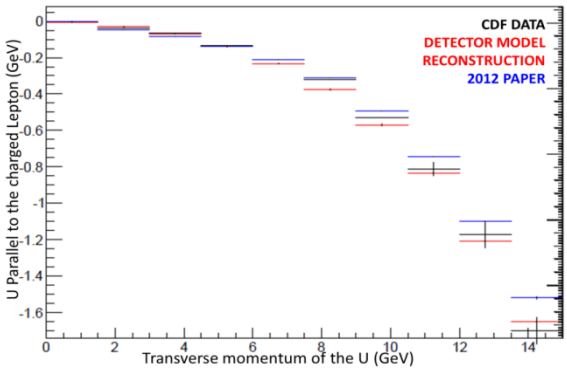

Figure 10: *The recoil of W events parallel to the lepton over a range of transverse U momenta.*

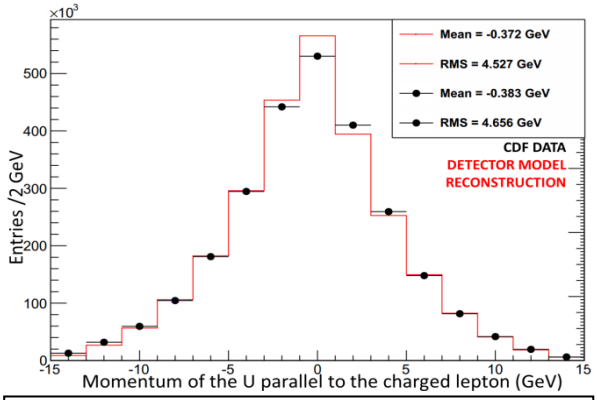

Figure 11: *Histogram comparing the reconstructed parallel momentum of the hadronic recoil in the detector model reconstruction (red) to the CDF data*[9] *(black).*

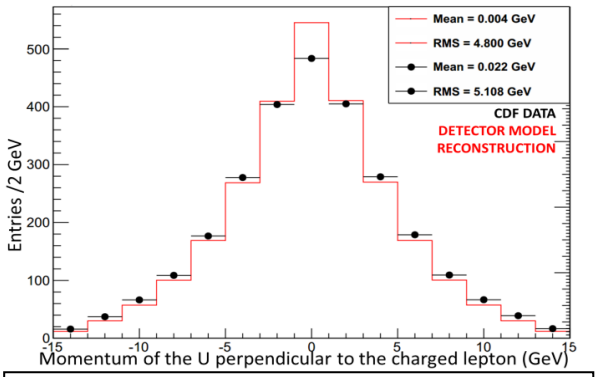

Figure 12: *Histogram showing the reconstructed perpendicular component of the momentum of the hadronic recoil for the detector model prediction (red) and the CDF data*[9] *(black).*

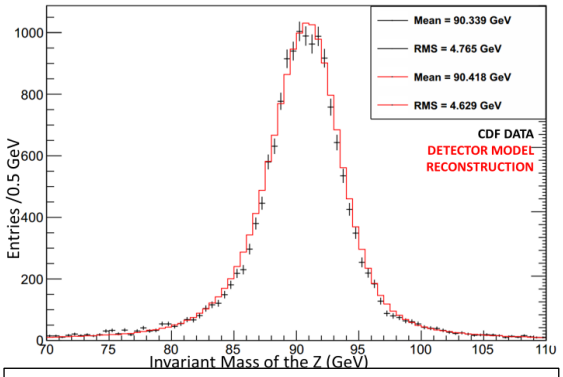

Figure 13: *A comparison of the prediction of the model and the CDFII experimental data[10] of the Z invariant mass.*

our model for Gaussian smearing of the lepton transverse momentum. Achieving the correct shape for each of these distributions is crucial, as it has been shown that a shift of M_W as small as 10 MeV can have a statistically significant impact on the shape of these distributions[8].

III. Investigating PDF Uncertainties

A. Mass fit

In order to study the of PDF uncertainties on M_W, we create templates within a chosen fit range for the transverse mass, for 401 values of M_W between 80 348 MeV and 80 448 MeV. We then fit each of these templates to our detector model to determine the best fit value of M_W. We do this by maximising the likelihood L given by

$$L = \prod_i^N \frac{e^{-m_i} m_i^{n_i}}{n_i!} \qquad (6)$$

where N is the number of bins in the fit region with m_i and n_i are the number of expected

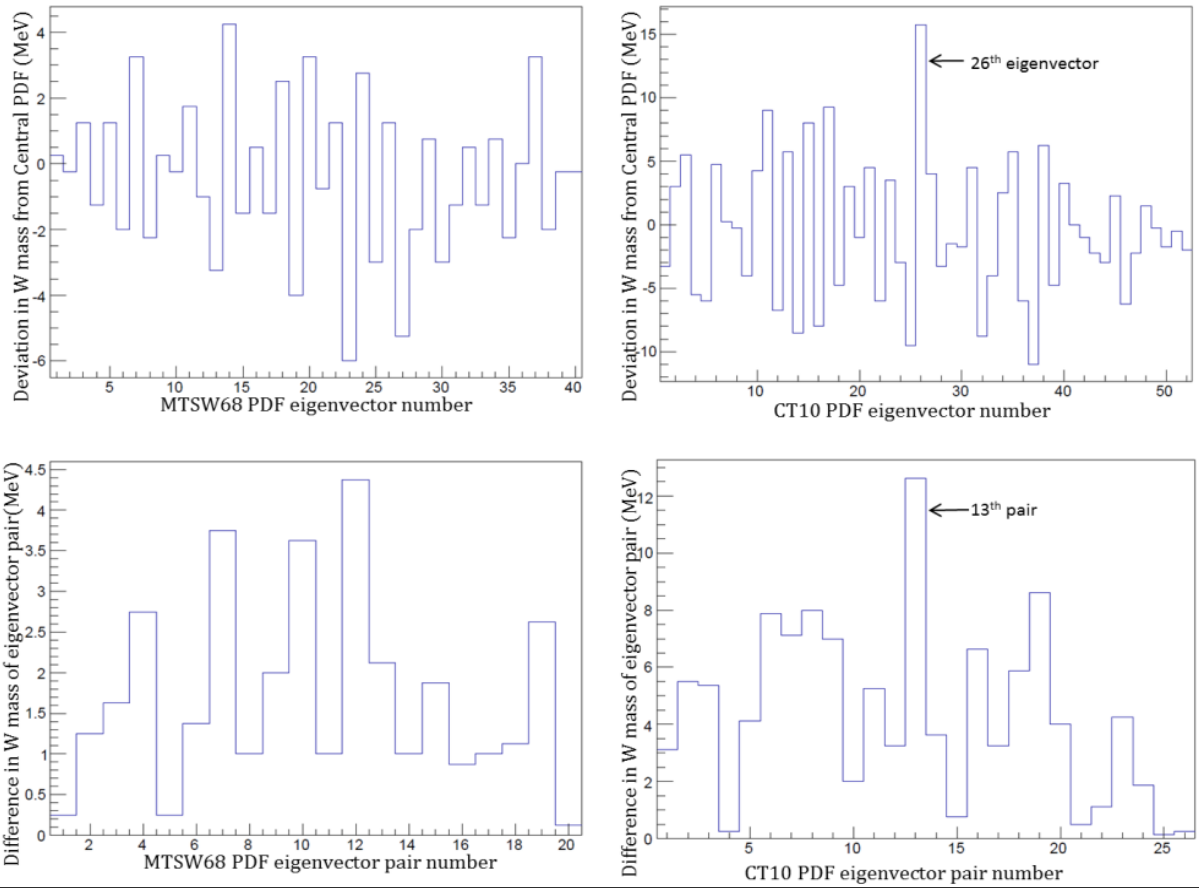

Figure 14: *The shift in M_W fit using the transverse mass for each eigenvector relative to the central PDF (top) and the difference between the two members of each eigenvector pair (bottom) for the MTSW68 PDF set (left) and the CT10 PDF set (right). Notice the large contribution from CT10 eigenvector 26, and its large disparity from eigenvector 25.*

entries for the template and the data respectively for the i^{th} histogram bin[2].

We repeat this process for each of the PDF eigenvectors in the CT10 and MTSW68 PDF sets. Figure 14 shows the shift in the M_W using the transverse mass as calculated by each eigenvector relative to the value calculated with the central PDF for these sets. We add the deviations in M_W for each PDF eigenvector of a given set in quadrature, to give the total PDF uncertainties on M_W, as shown in Table 4. Each PDF in these sets comes as one of a pair. The charts at the bottom of Figure 14 show the deviation in M_W between members of the same pair for each pair in the CT10 and MTSW68 sets. By fitting for M_W using the transverse momentum of the lepton and neutrino instead of the transverse mass, we obtain the values of total uncertainty in Table 5.

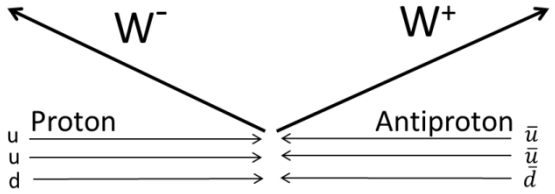

Figure 15: *The W^+ is boosted in the direction of the proton beam, and the W^- is boosted in the direction of the Antiproton beam.*

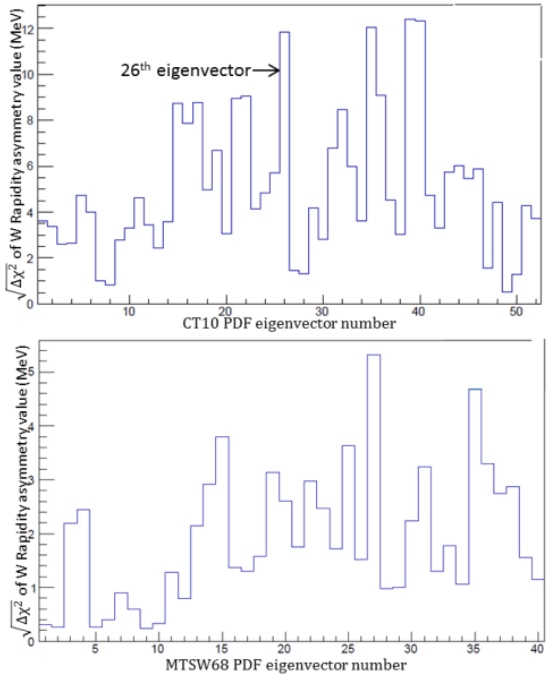

Figure 16: *The square root of the delta chi squared of the W rapidity asymmetry distribution for each PDF in the CT10 eigenvector set (above) and the MTSW68 eigenvector set (below), compared to the central PDF set.*

B. Measurements on Z rapidity and W Charge asymmetry

When a W^+ boson is produced in a proton anti-proton collision, its momentum will be boosted in the direction of the proton beam because the greater porportion of the momentum which an up quark carries relative to a down quark. Conversely, the momentum of a W^- boson produced in such a reaction will have it's momentum boosted in the direction of the anti-proton beam (Figure 15). We subtract the rapidity distribution of the W^- from the rapidity distribution of the W^+ to

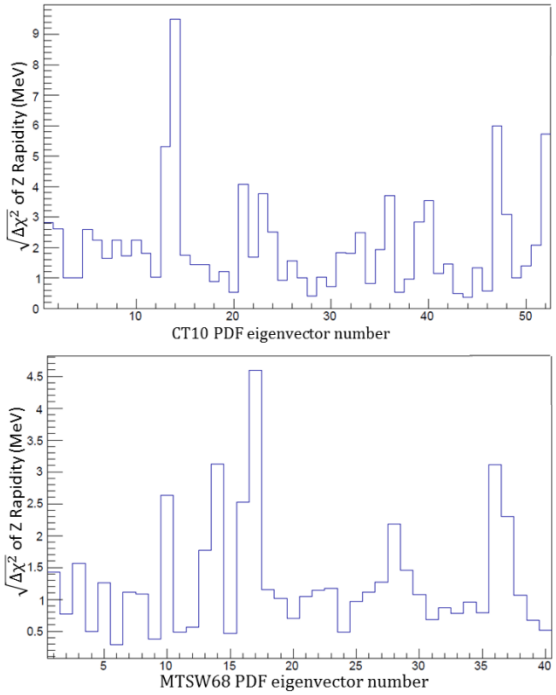

Figure 17: *The square root of the delta chi squared of the Z rapidity distribution for each PDF in the CT10 eigenvector set (above) and the MTSW68 eigenvector set (below) compared to the central PDF set.*

Energy range of calculation (GeV)	CDF Transverse mass MSTW68 σ (MeV)	CDF Transverse mass MSTW68 σ with raised cuts (MeV)	CDF Transverse mass CT10 σ (MeV)	CDF Transverse mass CT10 σ with raised cuts (MeV)
60 - 100	10.5	N/A	31.0	N/A
60 - 90	10.7	N/A	31.0	N/A
62.5 - 90	10.2	N/A	29.6	N/A
65 - 90	9.2	8.3	26.8	8.3
67.5 - 90	8.2	7.5	24.0	7.5
70 - 90	7.6	6.6	22.6	6.6
72.5 - 90	7.7	6.1	22.8	6.1
75 - 90	8.6	6.5	25.0	8.2
CDF value (65-90)	10	N/A	N/A	N/A

Table 4: *The total uncertainty on M_W using the MTSW68 and CT10 PDF sets for the transverse mass, with the model configured to CDF data.*

obtain a distribution for the the W charge asymmmetry as a function of rapidity. Measurements of this asymmetry can give us useful information about the up : down momentum ratio. We calculate the chi squared of the W charge asymmetry, defined as

$$\chi^2 = \sum_{bins} \frac{(N_{data} - N_{model})^2}{\sigma} \qquad (7)$$

where $N_{data} - N_{model}$ is the difference in the W charge asymmetry between the model and the data for each bin, and σ is the uncertainty on the bin. Figure 16 shows the square root of the change of the chi squared value of the W charge asymmetry distribution for each PDF eigenvector of the CT10 and MTSW68 PDF sets, compared to the chi squared for the central PDF for each set. Since Z–bosons are produced in proton-antiproton collisions by the annhialation of a quark and its antiquark, there is no such charge bias on the direction of the boson. Measurements of the distribution of Z rapidity therefore serve as symmetrical probe on each quark. Figure 17 shows the square root of the change of the chi squared value of the Z rapdidity distribution for each PDF eigenvector of the CT10 and MTSW68 PDF sets, compared to the chi squared for the central PDF.

Energy range of calculation (GeV)	CDF Lepton MSTW68 σ with original cuts (MeV)	CDF Neutrino MSTW68 σ with original cuts (MeV)	CDF Lepton MSTW68 σ with raised cuts (MeV)	CDF Neutrino MSTW68 σ with raised cuts (MeV)	CDF Lepton CT10 σ with original cuts (MeV)	CDF Neutrino CT10 σ with original cuts (MeV)	CDF Lepton CT10 σ with raised cuts (MeV)	CDF Neutrino CT10 σ with raised cuts (MeV)
30 - 55	11.6	10.8	N/A	N/A	34.6	31.5	N/A	N/A
30 - 48	11.3	11.2	N/A	N/A	33.7	32.3	N/A	N/A
31 - 48	10.7	10.5	N/A	N/A	31.9	30.5	N/A	N/A
32 - 48	9.9	9.8	8.7	8.4	30.1	28.6	26.6	24.6
33 - 48	9.2	9.1	8.1	7.8	28.2	26.7	24.9	23.0
34 - 48	8.6	8.7	7.4	7.2	26.7	25.4	23.2	21.2
35 - 48	8.4	8.5	6.8	6.8	26.0	24.8	22.0	20.0
36 - 48	8.4	8.7	6.6	6.5	26.3	25.2	21.5	19.5
CDF value (32-48)	9	11	N/A	N/A	N/A	N/A	N/A	N/A

Table 5: *The total uncertainty on M_W using the MTSW68 and CT10 PDF set for the lepton and neutrino transverse momenta, with the model configured to match CDF data.*

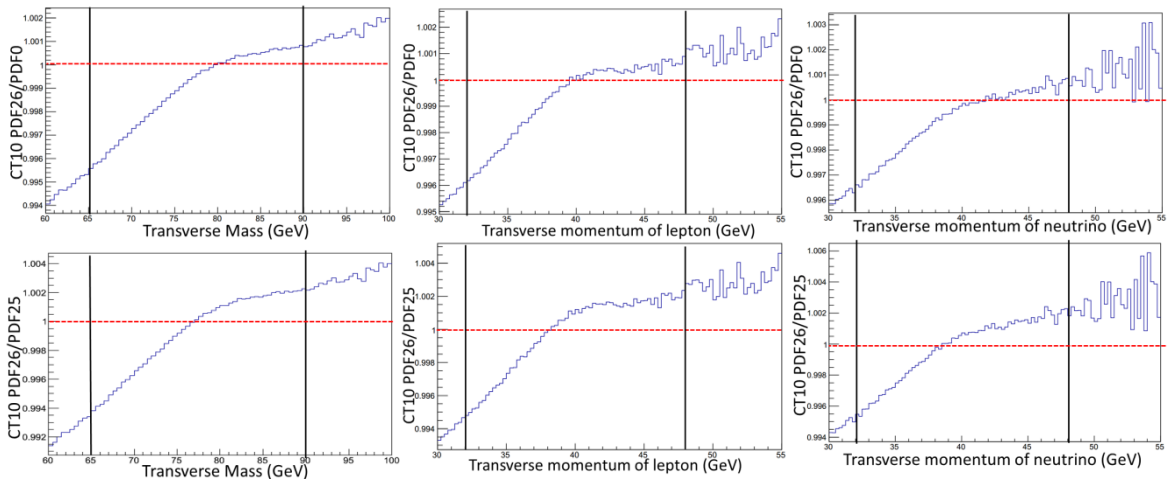

Figure 18: *Plots showing the ratio of the predictions of the CT10 PDF eigenvector 26 to that of the central PDF (top) and to its partner, PDF 25 (bottom), for the transverse mass (left) electron P_T (centre) and neutrino P_T (right).The fit range used in the CDF measurement is shown between the black vertical lines.*

C. Fit range for M_W

As the charts on the right-hand side of Figure 14 clearly demonstrate, the 26th eigenvector of the CT10 parton distribution function set deviates from the central PDF far more than the other PDFs in the set in its value for M_W. We investigate this phenomenon by plotting the ratio of the transverse mass predicted by PDF 26 compared with that predicted by the central PDF. We also produce similar ratio plots with PDF 25 (the eigenvector to which PDF 26 is paired) in place of the central PDF and repeat the process for electron and neutrino transverse momentum. All the ratio plots in Figure 18 share the common features of a large deviation at the low end of the spectrum. This feature motivates reducing the range for the mass fit. Tables 4 and 5 show the results for several fit ranges. For the CDF fit ranges, (65 GeV-90 GeV for M_T and 32 GeV-48 GeV for both P_T^l and P_T^ν) the uncertainties determined with our model closely resemble those calculated by the CDF collaboration[2]. This gives us confidence in the accuracy of our model. Tables 4 and 5 show the potential for reducing uncertainties by changing the fit range, these tables also show the results of investigations into the effects of increasing the lower bounds for the selection criteria for W events from; $P_T^l \geq$30 GeV, $P_T^\nu \geq$30 GeV, $M_T \geq$60 GeV, up to; $P_T^l \geq$32 GeV, $P_T^\nu \geq$32 GeV, $M_T \geq$64 GeV.

D. Prospects for ATLAS

In order to estimate the impact of PDF uncertainties on M_W measurements at the LHC, we generated a total of 102 million events $\sqrt{s}$ = 7 GeV using POWHEG. We found the total uncertainties (Tables 6 and 7) to be consistent with the CDF uncertainties. The ATLAS detector has the capability of

Energy range of calculation (GeV) / pseudorapidity range	Transverse mass MSTW68 σ (MeV)	Transverse Mass CT10 σ (MeV)
60 – 100 / |η|<1	11.2	30.1
65 – 90 / |η|<1	8.9	26.1
60 – 100 / |η|<2.5	3.5	12.3
65 – 90 / |η|<2.5	3.0	10.4

Table 6: *Total uncertainty on the MTSW68 and CT10 PDF sets for the transverse mass fit for MW using $\sqrt{s}$ = 7 TeV samples. Notice the dramatic drop in the uncertainties when the pseudorapidity range is increased.*

Energy range of calculation (GeV) / pseudorapidity range	Lepton MSTW68 σ (MeV)	Neutrino MSTW68 σ (MeV)	Lepton CT10 σ (MeV)	Neutrino CT10 σ (MeV)
30 – 55 / |η|<1	11.1	10.8	33.5	29.0
32 – 48 / |η|<1	9.7	9.7	31.5	28.6
30 – 55 / |η|<2.5	4.0	3.5	14.9	13.3
32 – 48 / |η|<2.5	3.2	2.8	10.8	9.8

Table 7: *The total uncertainty on M_W with the MTSW68 and CT10 PDF sets for the lepton and neutrino transverse momenta fits with $\sqrt{s}$ =7 TeV. Notice the dramatic drop in the uncertainties when the pseudorapidity range is increased.*

detecting charged leptons over a larger range of pseudorapidity; ATLAS can detect events with |η|<2.5 compared to |η|<1 at the CDF[8]. The effect on the uncertainty of increasing the range of pseudorapidity is displayed in Tables 6 and 7.

IV. Conclusions

Validations of the detector model with CDF data for the distributions of the electron and neutrino transverse momenta, the transverse mass, the hadronic recoil parallel and perpendicular to the charged lepton in W decay, resolution parallel and perpendicular to the Z, and the invariant mass of the Z (Figures 7 – 13) show our detector model to be significant. This allows us to make useful studies of factors which contribute to the PDF uncertainty in the M_W measurement. In particular, the inclusion of events with a greater range of pseudorapidity enabled by more advanced detectors such as ATLAS has a dramatic effect on the total PDF uncertainties as evidenced in Tables 6 and 7. Increasing the range of events from |η|<1 to |η|<2.5 can cut the PDF uncertainty by a factor of three. We see a strong dependence of the uncertainty on the fit range, particularly the lower bound of the fit range: Tables 4 and 5 show that the total uncertainties are inversely proportional the lower bound of the fitting range up to about 70 GeV for M_T and 35 GeV for P_T^l and P_T^ν. These appear to be the optimal lower bounds for the fit ranges. This result is reinforced by our investigations into the effects of raising the lower cut on transverse momenta: We raised the cuts on transverse lepton, transverse neutrino, and transverse mass, from 30 GeV, 30 GeV and 60 Gev respectively to 32 GeV, 32 GeV, and 64 GeV. This had the effect of reducing the uncertainty predicted by our model by around 1 MeV on average (Tables 4 and 5). Another result of the study is that it should be possible to further constrain the PDF uncertainties by W charge asymmetry and with the full CDF data set. Figures 16 and 17 show the deviations from the central PDF for the CT10 and MTSW68 sets for the W charge asymmetry and Z rapidity respectively. Further investigations into the eigenvectors which provide the majority of uncertainty might provide inspiration for future measurements to reduce the PDF uncertainty. One problem we highlighted but were not able to resolve during our experimentation with different fitting parameters was that the uncertainty on the lepton was larger than the uncertainty on the neutrino for many of the fitting boundaries. From the CDF data, and also from the fact that the neutrino data is derived from the lepton data, we would expect the uncertainty on the neutrino to be larger than that of the lepton, which suggests there could be some room for further refinements on the detector model and the fitting algorithm.

References

[1] T. Aaltonen et al. (CDF Collaboration). PRL **108,** 151803 (2012)

[2] T. Aaltonen et al. (CDF Collaboration) arXiv:1311.0894v1 (2013)

[3] A.D. Martin, W.J. Stirling, R.S. Thorne, G. Watt, Parton distributions for the LHC arXiv:0901.0002v3 (2009)

[4] More information on the PDF sets used in this project, as well as the PDF sets themselves can be found at https://lhapdf.hepforge.org.pdfsets

[5] C.Oleari arXiv:1007.3893 [hep-ph] (2010)

[6] C. Hays, A. Kotwal, O. Stelzer-Chilton, Y. Zeng, *Hadronic recoil modelling for the W boson mass measurement using 2.3fb^{-1} of CDFII data* (2013)

[7] A. Kotwal, C. Hays, Nuclear Instruments and Methods in Phys. Research A 729 25-35 (2013)

[9] T. Aaltonen et al. (CDF Collaboration) Phys. Rev. D **77,** 112001 (2008)

[8] G.Bossi, J.Rojo, and A.Vicini, Phys. Rev. D **83,** 113008 (2011)

[10] T. Aaltonen et al. (CDF Collaboration) Phys. Lett. B **692,** 232-239 (2010)

[11] J. Rojo, A. Vicini arXiv:13-9.1311v1 [hep-ph] (2013)

[12] T. Aaltonen et al. (CDF Collaboration) PRL **102,** 181801 (2009)